Science and Technology Indonesia
*e*-ISSN:2580-4391 *p*-ISSN:2580-4405
Vol. 8, No. 3, July 2023

Research Paper

# Analysis of Extreme Heat Land Surface Temperature at a Tropical City (1988-2022): A Study on the Variability of Hot Spot during El Niño Southern Oscillation (ENSO)

Oliver Valentine Eboy[1], Ricky Anak Kemarau[2*]

[1]*Geography Program, Faculty Of Social Science and Humanities, Universiti Malaysia Sabah, Jalan UMS, 88400, Kota Kinabalu, Sabah, Malaysia*
[2]*Earth Observation Center, Institute Of Climate Change, Universiti Kebangsaan Malaysia, 43600, Bangi, Selangor, Malaysia*
***Corresponding author**: rickykemarau@ukm.edu.my*

**Abstract**
Weather and climate in Malaysia, situated in Southeast Asia, are influenced by El Niño Southern Oscillation (ENSO), monsoons, Madden Julian Oscillation (MJO), and Indian Ocean Dipole (IOD). Previous studies on ENSO's impact on temperature lacked detailed spatial information due to limited meteorological stations and cost constraints. This study utilizes remote sensing techniques, employing Landsat satellite data and Oceanic Niño Index (ONI) data, to analyze the spatial pattern of extreme land surface temperature distribution during ENSO events. Preprocessing includes radiometric and atmospheric corrections before converting digital numbers to land surface temperature values. Results indicate increased hotspot areas (>30°C) during El Niño events, with respective hotspot areas of 89.32 km² and 97.8 km² in 2015 and 2016, and 61.23 km² and 59.73 km² during La Niña in August and October 2018. Heat concentration areas remained consistent during the 1998 El Niño (89.32 km²) and the 2011 La Niña (55.82 km²). These findings highlight ENSO's influence on altering hotspot distribution patterns. The increased hotspot area during El Niño events (34-36 km²) led to a 20-30% surge in electricity consumption as residents and offices in Kuching City, Sarawak, sought temperature regulation. This spatial information aids the government in identifying affected areas and implementing suitable measures to mitigate the impact of El Niño events.

**Keywords**
Spatial-temporal, Extreme Land Surface Temperature, ENSO

Received: 8 January 2023, Accepted: 29 May 2023
https://doi.org/10.26554/sti.2023.8.3.388-396

## 1. INTRODUCTION

Malaysia's geographical location within Southeast Asia makes it vulnerable to various climate phenomena, including the El Niño Southern Oscillation (ENSO), Madden Julian Oscillation (MJO), Indian Ocean Dipole (IOD), and monsoon patterns (Lin et al., 2018). El Niño events often lead to temperatures above the long-term average in countries such as Malaysia, Indonesia, Thailand, and Vietnam (Sum et al., 2016; Kemarau and Eboy, 2020b). However, there is still a lack of studies examining the local-scale impact of these events on land surface temperatures in tropical cities (Zhou et al., 2018). Currently, temperature measurements are predominantly taken at airport locations in Malaysia, limiting our understanding of the specific effects of El Niño on land surface temperature in different types of land cover, particularly in densely populated urban areas. Acquiring spatial information about the distribution of extreme heat is crucial for making informed policy decisions and implementing effective measures to mitigate the impacts of heat waves during El Niño. Furthermore, El Niño events can result in prolonged and severe droughts (Thirumalai et al., 2017). Particularly significant are the highest recorded temperature increases observed in Southeast Asia during the El Niño events of 1997-1998 and 2015-2016 (Chen et al., 2002). The World Health Organization WHO (2016) documented instances of extreme heat during the 2015-2016 El Niño event, which led to the deaths of over 2,200 people in Karachi, Pakistan (Iyengar, 2015), and over 2,000 deaths in several cities in India. Additionally, during the 2016 El Niño event, the city of Blythe in California, USA, experienced a record-breaking temperature of 51°C. These incidents underscore the significant threat that El Niño poses to human life, particularly in terms of the health risks associated with higher-than-normal or extreme heat (IPCC, 2014).

The occurrence of El Niño events, which often lead to droughts and dry weather, poses a significant health risk, particularly in urban areas. However, our current understanding of the temperature distribution resulting from ENSO incidents remains limited. Sum et al. (2016) emphasized the importance

of spatial information and the use of remote sensing methods to identify affected areas during ENSO events. This information is crucial for comprehending the future impact of ENSO. For instance, accurate spatial information, including location maps of affected areas, is invaluable to organizations such as the State Disaster Management Department, National Disaster Council, Natural Disaster Management Agency, charities, local governments, and the Ministry of Health. It enables them to provide targeted assistance, such as cloud seeding, to mitigate the impact of El Niño on affected populations. Reliable spatial data on hotspot areas also supports responsible parties in urban planning and local governance by allowing them to predict and implement infrastructure developments, such as green and blue areas, to mitigate the effects of El Niño on surface temperature and urban climates. To date, remote sensing technologies have predominantly focused on studying the effects of ENSO on sea surface temperatures, while studies examining the impact of ENSO on land surface temperature, particularly in relation to urban climates, have received less attention (Zhou et al., 2018). However, it is crucial to understand the Oceanic Niño Index (ONI) as an indicator for measuring the strength of ENSO and its effect on urban temperature (IPCC, 2014; Argüeso et al., 2015). Most studies utilizing remote sensing technology and Geoinformation Systems (GIS) have explored the effects of land-use changes on urban temperatures. Previous research has demonstrated that RS and GIS technologies are effective in mapping and observing the impacts of urban growth, which exacerbate the urban heat island effect and result in higher temperatures in urban areas compared to rural regions (Zhou et al., 2018).

## 2. EXPERIMENTAL SECTION

### 2.1 Location of Study, Dataset, and Method

#### 2.1.1 Location of Study

Kuching City (Figure 1) receives an average annual rainfall of 4,096 mm, with the highest recorded monthly rainfall reaching 485.4 mm (Kuok et al., 2019). The daily temperatures range from 23 to 32°C during the day (Kemarau and Eboy, 2021b). Kuching City was selected as the study location due to its historical experience with El Niño events. Mahmud (2018) reported that the city was impacted by El Niño in 1982-1983 and 1997-1998, resulting in a significant decrease in rainfall of 25–28%. This reduction in rainfall led to prolonged droughts and dry spells. Mahmud (2018) further noted that Kuching City experienced a 40% decrease in rainfall from May to October 1997 compared to the normal monthly average.

#### 2.1.2 Dataset and Method

In this research, Landsat 5 TM, 7 ETM, and 8 TIR OLI satellite data were utilized. The RS data were selected from the period 1988 to 2019, focusing on cloud-free imagery at the study location. A total of 37 Landsat data sets were downloaded from the website https://earthexplorer.usgs.gov/. Detailed information about the satellite data is discussed in the study highlights. The Oceanic Niño Index (ONI) was employed to identify El Niño and La Niña events (Halpert and Ropelewski, 1992). ONI serves as an indicator of the development and intensity of El Niño or La Niña in the Pacific Ocean. It represents a three-month sea surface temperature anomaly in the Niño zone 3.4, ranging from 5° North to 5° South and 120° to 170° West. El Niño is defined as the average sea surface temperature over three months with an anomaly of ≥ 0.5°C, while La Niña is defined as the average sea surface temperature over three months with an anomaly of ≤ -0.5°C (NOAA Climate Prediction Center, 2019). The strength of ENSO is classified into five categories based on the surface temperature anomaly: weak (0.5-0.9), moderate (1.0-1.4), strong (1.5-1.9), and very strong (≥ 2.0) for El Niño events, and vice versa for La Niña events. Before converting the digital numbers to land surface temperature, the RS data underwent pre-processing, including geometric, radiometric, and atmospheric corrections, as illustrated in Figure 2. The conversion from digital numbers to land surface temperature followed a specific algorithm outlined by Kemarau and Eboy (2021a).

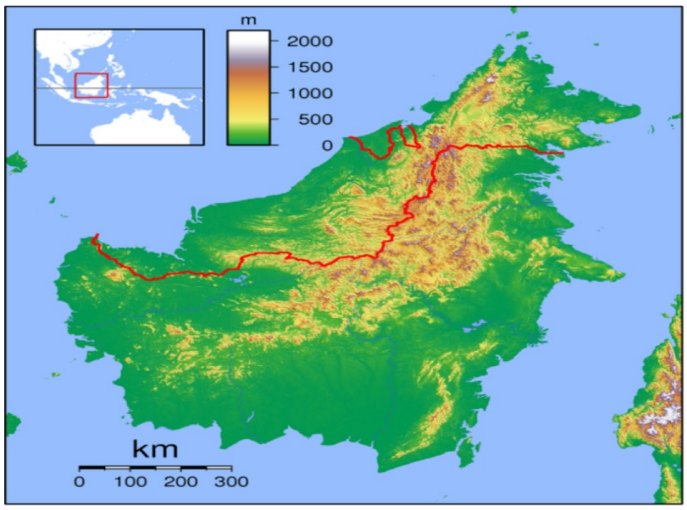


**Figure 1.** Location of Study

This study utilizes GIS analysis to identify hotspots, which are areas with temperatures exceeding 30 degrees Celsius based on the Land Surface Temperature (LST) during El Nino and La Nina events. The selection of hotspots exceeding 30 degrees Celsius is based on the classification method proposed by Baum et al. (2009). Their research suggested that human beings may experience slight discomfort when exposed to temperatures above this threshold. GIS analysis refers to the use of Geographic Information Systems, which are computer-based tools for collecting, managing, and analyzing spatial data. In this study, GIS is employed to analyze temperature data and identify specific areas that experience higher temperatures during El Nino and La Nina events. These events are natural climate phenomena that occur in the Pacific Ocean and can have significant impacts on global weather patterns. The term "hotspot"

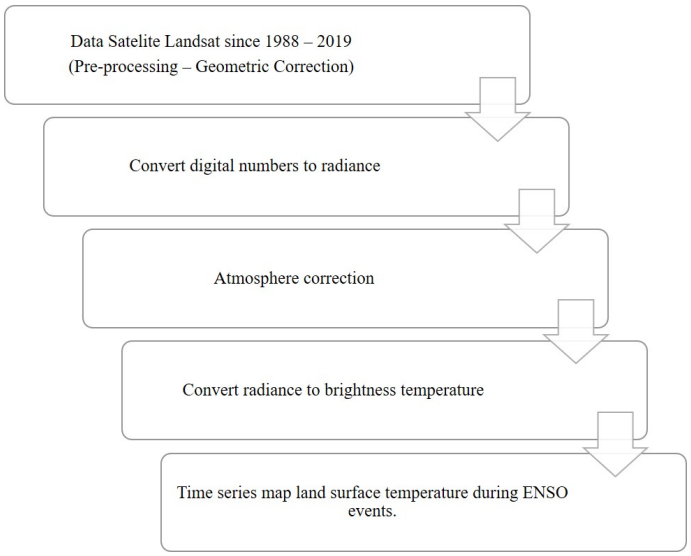


**Figure 2.** Flow Method Applied to Achieve the Objective of the Study

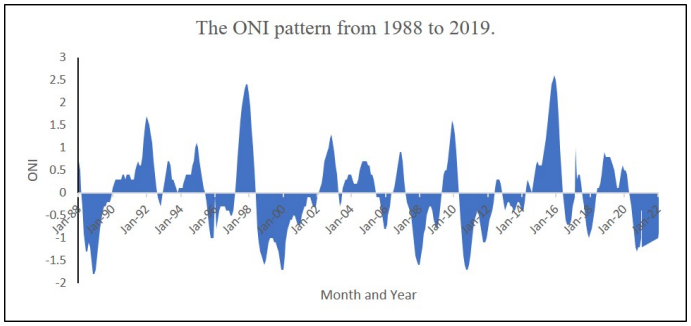


**Figure 3.** The ONI Pattern from 1988 to 2019

is used to describe areas that have temperatures exceeding 30 degrees Celsius. This threshold is chosen as it is believed to be a point where humans may start to experience some level of discomfort. The classification method developed by Baum et al. (2009) is referenced for identifying such hotspots. Their research likely provided specific criteria or guidelines for determining these areas based on temperature data. The study aims to locate and map these hotspots using GIS analysis. By identifying areas with temperatures exceeding 30 degrees Celsius during El Nino and La Nina events, researchers can gain insights into the spatial distribution and intensity of these hotspots. This information can be valuable for understanding the potential impacts of these climate phenomena on human activities, ecosystems, and other relevant factors.

## 3. RESULTS AND DISCUSSION

### 3.1 El Nino and La Nina Classification

ONI is used to measure the magnitude of ENSO strength, as illustrated in Figure 3. ONI ≥ 0.5 indicates El Niño, while ONI ≤ -0.5 indicates La Niña.

Table 1 lists the years of La Niña and El Niño occurrences during the period 1988-2019, based on the classification of ENSO events where ONI ≥ 0.5 indicates El Niño and ONI ≤ -0.5 indicates La Niña.

**Table 1.** List of Years of La Nina and El Nino During the Period 1988-2019

| La Niña | El Niño |
|---|---|
| 1989 | 1991/1992 |
| 1996 | 1994 |
| 1999 | 1997/1998 |
| 2005 | 2002/2003 |
| 2007/2008 | 2004 |
| 2010 | 2006 |
| 2011 | 2009 |
| 2018 | 2015/2016 |

According to NOAA, the magnitude of El Niño and La Niña strength is classified based on sea surface temperature anomalies into four categories: weak (0.5-0.9), moderate (1.0-1.4), strong (1.5-1.9), and very strong (≥ 2.0). Positive values (ONI ≥ 0.5) refer to El Niño, while negative values (≤ -0.5) refer to La Niña. This study involved data from 37 Landsat satellites and 237 MODIS data to analyze surface temperature anomalies. However, the displayed surface temperature maps only highlight strong and very strong anomalies during La Niña and El Niño events. This means that the El Niño events analyzed in this study only occurred in 1997-1998 and 2015-2016, while La Niña events occurred in 1989, 1999, 2010-2011, and 2017-2018. Therefore, this study focuses only on ENSO events with ONI >1 and <-1. The study also categorizes the study location into industrial and urban zones to understand the effects of ENSO events on the temperature in Kuching City, Sarawak, using remote sensing data. The industrial and urban areas were chosen because previous studies found that these areas constitute urban heat islands (with higher temperatures compared to vegetated and water-covered areas). La Niña is a weather pattern characterized by a cooling of the equatorial Pacific Ocean, which leads to specific atmospheric changes. This phenomenon can have significant impacts on global commodity markets, affecting various regions differently. La Niña can result in dry conditions and drought in certain areas, adversely affecting cropland and agricultural productivity. Conversely, it can bring excessive rainfall and flooding to other regions. These contrasting weather conditions associated with La Niña can have significant implications for agriculture, water resources, and overall economic stability in affected areas.

#### 3.1.1 Relationship between ONI and LST

Figure 4 depicts a notable positive correlation between the Oceanic Niño Index (ONI) and surface temperature derived from Landsat satellites, with a correlation coefficient of 0.71. This positive relationship indicates a direct proportion, imply-

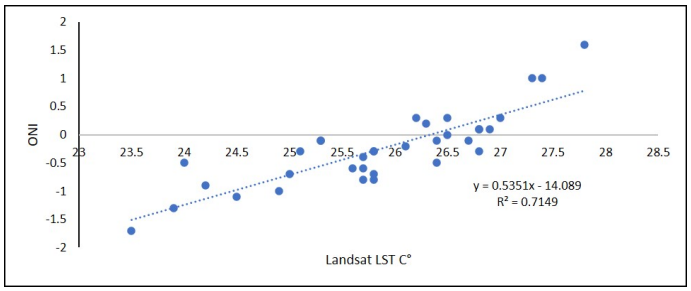


**Figure 4.** The Correlation Between ONI and Surface Temperature in Kuching City Using Landsat Satellite Data

ing that an increase in ONI corresponds to a rise in surface temperature.

Table 2 presents the results of linear regression analysis, aiming to examine the impact of ENSO on surface temperature in Kuching, Sarawak, and using Landsat satellite data.

Table 2 displays the regression coefficients for R and $R^2$. An R-value of 0.75 indicates a strong correlation between ONI and surface temperature as observed by the Landsat satellite. An $R^2$ value of 0.57 suggests that 57% of the variability in surface temperature can be explained by ONI. In other words, ONI accounts for 57% of the influence on temperature.

Table 3 presents the analysis of variance (ANOVA) results, which assess the significance of the relationship between the dependent and independent variables. It tests the appropriateness of using the independent variable to understand the variations in the dependent variable.

Table 1 demonstrates the efficacy of the regression model in effectively understanding the dependent variables, highlighting the significance of regression analysis. A p-value <0.0005, which is less than 0.05, indicates statistical significance. This suggests that the regression model aligns well with the study data.

Based on Figure 5, the left side of the figures indicates the dates when Landsat data was recorded during El Niño events, with ONI values of 1.1 for the figure above left, 1 for the figure in the middle left, and 1 for the figure at the bottom left. Conversely, the right side of the figures represents temperature distribution maps during La Niña, corresponding to negative ONI values of -1 for the figure above right, -1 for the figure in the middle right, and -1.1 for the figure at the bottom right. Figure 4 displays a temperature distribution map during El Niño, where most study locations are depicted in yellow shades, indicating above-normal surface temperatures. On the other hand, during the La Niña events in Kuching City, Sarawak, the temperature map shows bluish hues, representing lower local temperatures compared to the El Niño period. The identification of hotspot areas was further categorized into urban and industrial zones. It is observed that during El Niño, the number of hotspot areas in Kuching City is higher than during La Niña. For example, during an El Niño event, zones B, C, D, E, F, G, H, I, and J consistently experience temperatures above 30°C,

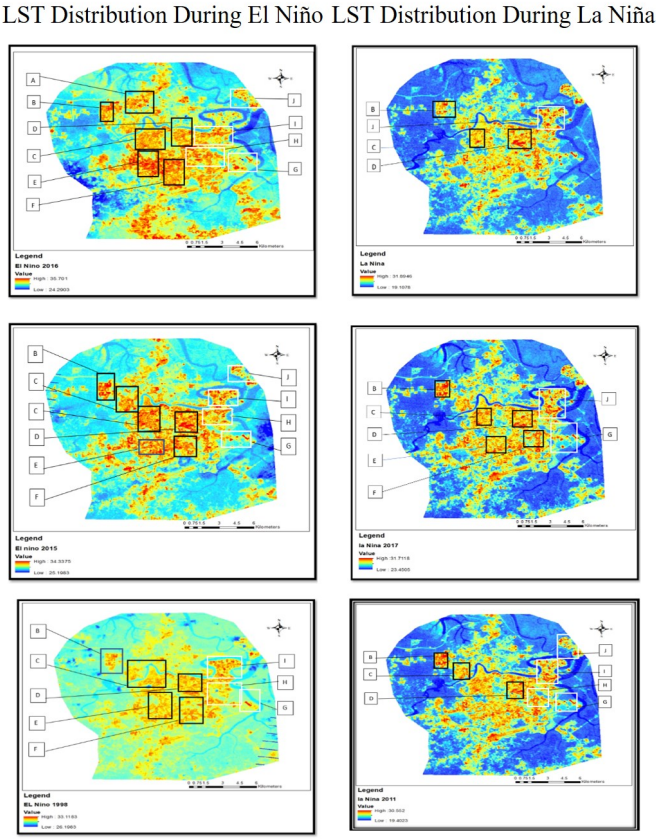


**Figure 5.** Map Illustrating Temperature Distribution During El Niño and La Niña Events

causing discomfort to the population, as noted by Baum et al. (2009). This occurrence is more pronounced during El Niño compared to La Niña, as depicted in Figure 5. To provide another example, referring to Figure 4, during El Niño, the hot focus areas encompass zones B, C, D, E, and F (urban areas), as well as G, H, and I (industrial areas), totaling 8 hot focus zones. In contrast, during La Niña, there are 7 hot focus zones, namely B, C, D, G, H, I, and J. Figure 5 illustrates the expansion of hotspots, representing areas with temperatures exceeding 30°C, during both La Niña and El Niño events. To further understand the impact of ENSO events on temperature distribution in Kuching City, Sarawak, this study analyzes the statistical values of maximum, minimum, and average temperatures using Landsat satellite data. Table 4 provides comprehensive information on these statistical values for maximum, minimum, and average temperatures during both La Niña and El Niño events. The table presents detailed data on temperature variations derived from Landsat satellite remote sensing (RS) data, which offers the advantage of minimal cloud coverage. The distinctions in average, maximum, and minimum temperatures are based on the ONI values, with values below -1 indicating La Niña events and values above 1 indicating El Niño events in Kuching City, Sarawak. The following paragraph provides a detailed explanation of the differences in the statistical values

**Table 2.** Linear Regression Analysis of the Influence of ENSO on Surface Temperature in Kuching City, Sarawak, Based on Landsat Satellite Data

| Model | R | $R^2$ | Adjusted $R^2$ | Std. Error for the Estimation |
|---|---|---|---|---|
| 4 | 0.755 | 0.570 | 0.556 | 0.66631 |

a) Predictor: (Constant) ONI Index

**Table 3.** ANOVA Results for the Regression Analysis of the Impact of ENSO on Surface Temperature Observed by the Landsat Satellite

| Model | Sum of Squares | Df | Mean Square | F | Sig |
|---|---|---|---|---|---|
| Regression | 18.810 | 1 | 18.810 | 42.368 | 0.000 |
| Residual | 14.207 | 32 | 0.44 | | |
| Total | 33.017 | 33 | | | |

a) Dependent Variable: LST Landsat b) Predictor: (Constant): ONI

of maximum, minimum, and average temperatures obtained from Landsat satellite RS data during the La Niña and El Niño events in Kuching City, Sarawak.

Table 4 presents the statistical information values for each ONI difference in the selected data, considering ONI values exceeding ± 1 and no cloud coverage at the study location. Table 4 displays the average, maximum, and minimum temperatures during El Niño, which are higher compared to La Niña. For instance, during ONI 1.1 in April 1998, which coincided with El Niño, the average temperature was 27.81°C, while during ONI -1.1 in November 2011, which occurred during La Niña, the average temperature was 24.91°C. A similar trend can be observed in the data recorded in July 2015, with an average temperature of 26.90°C during El Niño (ONI 1.1), higher than the average temperature during La Niña, which was 24.2°C (ONI -1). The same pattern can be observed for the maximum and minimum temperature values. For El Niño, the maximum temperature reached as high as 35.90°C, while the minimum temperature dropped to 24.29°C. In comparison, during La Niña, the maximum temperature recorded was 31.39°C, and the minimum temperature was 19.10°C, occurring in July 2016 (El Niño, ONI 1) and non-October 2017 (La Niña) respectively. Table 4 further elucidates the differences in maximum, minimum, and average temperatures. The average temperature exhibits a difference ranging from 2.10°C to 2.90°C. The difference in maximum values ranges from 2.32°C to 4.51°C, while the difference in minimum values ranges from 2.74°C to 6.77°C. ENSO events have a significant influence on local temperatures, and remote sensing (RS) technology enables the recording and provision of valuable information on hot and cold focal spaces during La Niña and El Niño events, as depicted in Figure 5. Before the advent of RS technology, predicting phenomena like floods, earthquakes, hurricanes, and droughts was challenging. Researchers worldwide are actively working on developing specific models to alert the public and better prepare for unexpected events such as the ENSO incident. By utilizing RS data, it becomes possible to predict natural disasters and enable affected areas, including hotspots, to enhance preparedness in Kuching, Sarawak. This proactive approach helps prevent property damage and save lives during events like droughts and floods.

### 3.1.2 Areas of Hotspot (Land Surface Temperatures Above 30 °C) During La Nina and El Nino Event

Figure 6 illustrates the distribution of surface temperatures, highlighting regions with land surface temperatures above 30°C (represented by the red color), during the occurrences of La Niña and El Niño events. Based on the observations, it is evident that the total area of hotspots during the El Niño event is greater than that during the La Niña event. Figure 6 provides a detailed analysis of the disparities in hotspot areas between the La Niña and El Niño events.

Based on Figure 7, it is evident that the hotspot area during the El Niño event is higher than that during the La Niña event. For the El Niño events of 2015 and 2016, the hot focus areas covered an area of 89.32 km² and 97.8 km², respectively, in contrast to the La Niña event in August 2018 and October 2018, where the hot focus areas measured 61.23 km² and 59.73 km², respectively. This consistent pattern of heat concentration in the area persisted during the 1998 El Niño event, which exhibited a hot focus area of 89.32 km², compared to the La Niña event in 2011, which had an area of 55.82 km².

These results demonstrate the impact of ENSO in altering the patterns of hot focus areas. The increase in hotspot area of 34 to 36 km² during the El Niño event corresponded to a rise in electricity consumption of 20-30% above normal levels, as a means to balance the temperatures in residential and office areas in Kuching City, Sarawak. These findings align with previous studies conducted by Cai et al. (2018), Lin et al. (2018), and Drosdowsky and Wheeler (2014), which have highlighted that El Niño events can contribute to a global temperature increase. This global temperature rise indirectly influences local temperatures, particularly at the study location. Additional support for this phenomenon can be found in the works of

**Table 4.** La Niña and El Niño Land Surface Temperature Statistics for the Landsat Satellite in Kuching City

| ONI Value | Statistic Value LST (°C) | ONI Value | Statistic Value LST (°C) | LST Difference (°C) |
|---|---|---|---|---|
| -1 (La Niña) | Maximum (31.39) | 1 (El-Niño) | Maximum (35.90) | Maximum (4.51) |
| | Minimum (19.10) | | Minimum (24.29) | Minimum (5.29) |
| | mean (24.8) | | mean (26.90) | mean (2.10) |
| -1 (La Niña) | Maximum (31.71) | 1.1 (El-Niño) | Maximum (34.33) | Maximum (2.62) |
| | Minimum (23.45) | | Minimum (25.19) | Minimum (2.74) |
| | Mean (24.2) | | Mean (26.72) | mean (2.52) |
| -1.1 (La Niña) | Maximum (30.55) | 1 (El-Niño) | Maximum (33.31) | Maximum (2.76) |
| | Minimum (19.42) | | Minimum (26.19) | Minimum (6.77) |
| | mean (24.91) | | Mean (27.81) | Mean (2.9) |

Tan et al. (2021), Moura et al. (2019), and Yang et al. (2018), Yu et al. (2015) concluded that the influence of local climate does not affect the impact of El Niño warming when it is dominant, specifically during the mature stage. This helps explain why the statistical values of maximum, minimum, and average temperatures, as well as the extent of hotspot areas, are higher around Kuching City during El Niño compared to La Niña. According to the data presented in Table 4, the average temperature during the El Niño events of 1997 and 1998 was 27.8°C and 26.9°C respectively, whereas, during the La Niña events in November 2011 and September 2010, it was 24°C. This indicates a temperature difference of 2°C to 3°C between El Niño and La Niña incidents. Kemarau and Eboy (2021a) stated that rainfall decreases during El Niño events, leading to a rise in temperature, while rainfall is abundant during La Niña events, resulting in a drop in temperature in Kuching City. They further reported that El Niño causes a temperature rise ranging from 0.5°C to 1.5°C, while La Niña leads to a temperature decrease of 0°C to 1.2°C. This accounts for the higher occurrence of hotspots during El Niño events compared to La Niña events. However, the findings of this study differ from those of Moura et al. (2019) who conducted research in the Amazon and reported a temperature difference of 7.5-8°C between El Niño and La Niña events using MODIS data.

The disparity in the effect of ENSO occurrences on temperature, as observed by Moura et al. (2019), can be attributed to factors such as landform variations, where temperatures in lowland areas tend to be higher than those in regions closer to the Andes Mountains. Kogan and Guo (2017) utilized MODIS data to examine the impact of El Niño on global temperature and worldwide plant systems. Their findings revealed that El Niño results in a temperature increase of 0.5-2.50°C, varying depending on the location. These results closely align with the findings of the current study. The disparity in temperature change can be attributed to factors such as the shape of the Earth's surface and the specific location, as stated by Siniarovina (2021). This highlights the effectiveness of remote sensing (RS) techniques in identifying the effects of El Niño and La Niña events on temperature distribution, specifically in Kuching City, Sarawak.By employing Landsat satellite data, the study investigated the influence of ENSO on the city. The selected data, which indicated strong ENSO strength values of -1 (La Niña) and 1 (El Niño), revealed a temperature increase ranging from 2.10-2.80°C. This temperature rise demonstrates the impact of urban heat islands during El Niño, amounting to 1.30-1.50°C after accounting for the overall temperature rise pattern in Malaysia, excluding the influence of urban heat, as studied by Tan et al. (2021). The findings of this study align with Tawang et al. (2003) research, which reported temperature increases of 0.1-1.9°C in Kedah and 0.1-2.4°C in Perlis during the 1997 El Niño, using meteorological data. Through RS techniques, it was identified that downtown and industrial areas act as hotspots, with surface temperatures exceeding 30°C, causing discomfort to humans (Baum et al., 2009). Conversely, areas in proximity to bodies of water and regions covered with vegetation exhibit lower temperatures and serve as cold spots. Industrial areas, represented by zones H, I, J, and K, are among the identified hotspots and record the highest temperatures due to high heat emissions (Li et al., 2011; Buyantuyev and Wu, 2010). Similarly, urban areas, depicted as black squares (zones B, C, D, E, F, and G), experience elevated surface temperatures due to the presence of buildings and man-made structures,

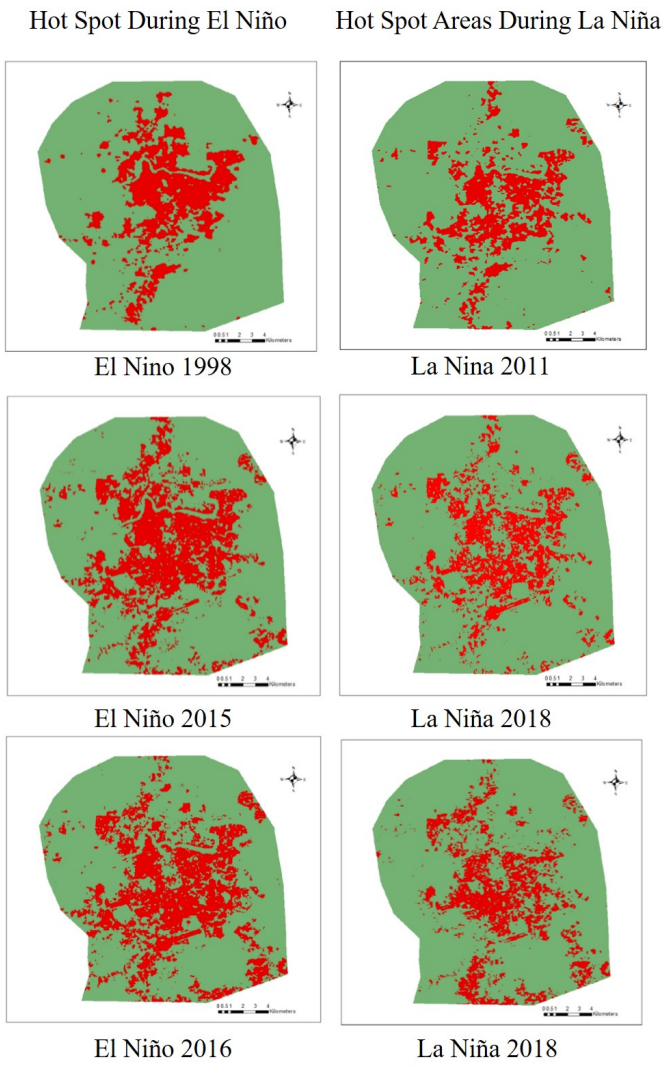


**Figure 6.** Distribution of Surface Temperatures Above 30°C (Represented by the Red Color), During the Occurrences of La Niña and El Niño Events

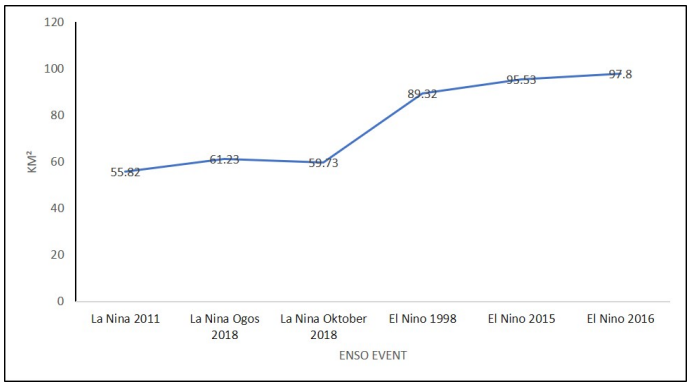


**Figure 7.** Comparison of Hotspot Areas (Areas with Surface Temperatures Above 30 °C) During El Niño and La Niña Events Using Landsat Satellite Data

exacerbating urban heat islands (Kemarau and Eboy, 2021b; Xu et al., 2013; Zhou et al., 2018). The anthropogenic contribution to urban heat islands, particularly through the use of indoor air conditioning, is significant, especially in downtown areas (Parker, 2010). Furthermore, Kemarau and Eboy (2021a) assert that emissions of carbon dioxide ($CO_2$) and carbon monoxide (CO) from industrial areas contribute to ambient temperature rise. The study also identifies water bodies and vegetation as cold spots, exhibiting the lowest temperatures. Previous studies by Zhang et al. (2016), Berger et al. (2017), and Yang et al. (2017) have demonstrated that plants and water bodies can mitigate surface temperatures in urban areas. This explains the presence of cold spots around bodies of water and vegetation, such as the Sarawak River, wetlands, and botanical gardens like the Bandar Budaya Forest. Furthermore, limited research has focused on the role of water bodies in mitigating temperature increases caused by urban heat islands. Studies by Zhang et al. (2016) and Kemarau and Eboy (2020a) employed the Normalized Water Difference Index (NDWI) and Land Water Surface Index (LWSI) respectively to examine the relationship between water bodies and surface temperature in urban areas. These studies have consistently found a positive correlation between the selected water body indices and temperature. In other words, an increase in the index value corresponds to a decrease in temperature. Additionally, the distance between water bodies or shorelines and green areas influences surface temperature. Proximity to water sources leads to lower surface temperatures when accompanied by lush vegetation (Kemarau and Eboy (2020a); Cai et al. (2018)). This implies that urban areas close to plants and water bodies experience lower temperatures compared to areas further away. Kemarau and Eboy (2020a) also suggested that future construction efforts should prioritize the planting of landscaping plants and designate strategic areas as recreational spaces for Kuching City residents, such as jungle trekking. Additionally, they proposed the implementation of environmentally friendly construction practices, such as green technology, to mitigate the impact of urban heat islands and ENSO on the temperature in the study area (Kemarau and Eboy, 2021a).

## 4. CONCLUSION

In summary, this study highlights the influence of ENSO on temperatures in Kuching City. El Niño events result in higher temperatures compared to La Niña events, with town areas and industrial zones identified as hotspots. Remote sensing data reveals increased hotspot areas during El Niño events, primarily in town areas and industrial zones, where elevated temperatures persist even during La Niña events due to urbanization and human activities. Cold concentration areas are found near water bodies and plants, naturally contributing to lower temperatures. The practical implications of these findings are significant, raising public awareness and inspiring proactive measures to mitigate urban heat and ENSO impacts. The spatial data obtained can inform the community about health and comfort concerns, with varying energy consumption

across different areas. Stakeholders, including urban planners, policymakers, and local power companies, can utilize this information to make informed decisions regarding infrastructure, construction practices, and eco-friendly buildings for a sustainable future.

## 5. ACKNOWLEDGMENT

The authors would like to express their gratitude to the Malaysia Meteorology Department for providing valuable data that contributed to the findings of this study. Additionally, we extend our appreciation to NASA (National Aeronautics and Space Administration) and NOAA (National Oceanic and Atmospheric Administration) for their data contributions, which were instrumental in the research process. Their provision of data has been crucial in enhancing our understanding of the impact of ENSO on temperature patterns in Kuching City.

## REFERENCES

Argüeso, D., J. P. Evans, A. J. Pitman, and A. Di Luca (2015). Effects of City Expansion on Heat Stress Under Climate Change Conditions. *PLoS one*, **10**(2); 0117066

Baum, S., S. Horton, D. Low Choy, and B. Gleeson (2009). Climate Change, Health Impacts and Urban Adaptability: Case Study of Gold Coast City. *Research Monograph*, **11**; 68

Berger, C., J. Rosentreter, M. Voltersen, C. Baumgart, C. Schmullius, and S. Hese (2017). Spatio-temporal Analysis of The Relationship Between 2d/3d Urban Site Characteristics and Land Surface Temperature. *Remote Sensing of Environment*, **193**; 225–243

Buyantuyev, A. and J. Wu (2010). Urban Heat Islands and Landscape Heterogeneity: Linking Spatiotemporal Variations in Surface Temperatures to Land-cover and Socioeconomic Patterns. *Landscape Ecology*, **25**; 17–33

Cai, Z., G. Han, and M. Chen (2018). Do Water Bodies Play an Important Role In the Relationship Between Urban Form and Land Surface Temperature? *Sustainable Cities and Society*, **39**; 487–498

Chen, C. C., B. McCarl, and H. Hill (2002). Agricultural Value of ENSO Information Under Alternative Phase Definition. *Climatic Change*, **54**(3); 305–325

Drosdowsky, W. and M. C. Wheeler (2014). Predicting the Onset of the North Australian Wet Season with the POAMA Dynamical Prediction System. *Weather and Forecasting*, **29**(1); 150–161

Halpert, M. S. and C. F. Ropelewski (1992). Surface Temperature Patterns Associated with the Southern Oscillation. *Journal of Climate*, **4**; 577–593

IPCC (2014). *Intergovernmental Panel Climate Change*. IPCC

Iyengar, R. (2015). *A Heat Wave in Pakistan Has Killed Around 140 People*. Time

Kemarau, R. A. and O. V. Eboy (2020a). Land Coverage Indices and Its Impact on Land Surface Temperature Pattern in Small Medium Sizes, Kota Kinabalu City for The Year 1991, 2011 and 2018. *Journal of Built Environment, Technology and Engineering*, **7**; 30–35

Kemarau, R. A. and O. V. Eboy (2020b). Urbanization and It Impacts to Land Surface Temperature on Small Medium Size City For Year 1991, 2011 And 2018: Case Study Kota Kinabalu. *Journal of Borneo Social Transformation Studies (JOBSTS)*, **6**(1); 5–15

Kemarau, R. A. and O. V. Eboy (2021a). Application of Remote Sensing on El Niño Extreme Effect in Normalized Difference Vegetation Index (NDVI) and Normalized Difference Water Index (NDWI). *Malaysian Journal of Applied Sciences*, **6**(1); 46–56

Kemarau, R. A. and O. V. Eboy (2021b). The Influence Of El Niño Southern Oscillation on Urban Heat Island Formation at Tropical City: Case of Kuching City, Sarawak. *GEOGRAFIA. Malaysian Journal of Society and Space*, **17**(4); 288–304

Kogan, F. and W. Guo (2017). Strong 2015–2016 El Niño and Implication to Global Ecosystems From Space Data. *International Journal of Remote Sensing*, **38**(1); 161–178

Kuok, K. K., S. M. Kueh, and P. C. Chiu (2019). Bat Optimisation Neural Networks for Rainfall Forecasting: Case Study for Kuching City. *Journal of Water and Climate Change*, **10**(3); 569–579

Li, J., C. Song, L. Cao, F. Zhu, X. Meng, and J. Wu (2011). Impacts of Landscape Structure on Surface Urban Heat Islands: A Case Study of Shanghai, China. *Remote Sensing of Environment*, **115**(12); 3249–3263

Lin, L., C. Chen, and M. Luo (2018). Impacts Of El Niño–southern Oscillation on Heat Waves in the Indochina Peninsula. *Atmospheric Science Letters*, **19**(11); e856

Mahmud, M. (2018). Peristiwa El Nino dan Pengaruh IOD Terhadap Hujan di Malaysia. *e-BANGI*, **13**(2); 166–177

Moura, M. M., A. R. Dos Santos, J. E. M. Pezzopane, R. S. Alexandre, S. F. da Silva, S. M. Pimentel, M. S. S. de Andrade, F. G. R. Silva, E. R. F. Branco, and T. R. Moreira (2019). Relation Of El Niño And La Niña Phenomena to Precipitation, Evapotranspiration and Temperature in the Amazon Basin. *Science of the Total Environment*, **651**; 1639–1651

NOAA Climate Prediction Center (2019). *Cold and Warm Episodes by Season*. Database of the Climate Prediction Center, National Weather Service, U.S. Department of Commerce

Parker, D. E. (2010). Urban Heat Island Effects on Estimates of Observed Climate Change. *Wiley Interdisciplinary Reviews: Climate Change*, **1**(1); 123–133

Siniarovina, A. U. S. (2021). *Impact of ENSO Events on Temperature in the City of Kuching, Sarawak*. Interview

Sum, L. P., T. M. Latif, T. Serin, K. H. Maidin, A. Q. Al-Amin, J. Liew, S. M. Alatas, L. C. Hur, S. Wong, and F. N. Ashikin (2016). El Niño-a Review of Scientific Understanding and the Impacts of 1997/98 Event In Malaysia. *A Report Prepared by the Task Force On El Niño For the Academy of Sciences Malaysia September*

Tan, M. L., L. Juneng, F. T. Tangang, J. X. Chung, and

 

R. Radin Firdaus (2021). Changes in Temperature Extremes and Their Relationship With Enso in Malaysia From 1985 to 2018. *International Journal of Climatology*, **41**; 2564–2580

Tawang, A. b., T. A. b. T. Ahmad, et al. (2003). *Stabilization of Upland Agriculture Under El Nino-induced Climatic Risks: Regional and Farm Level Risk Management and Coping Mechanisms in the Kedah-perlis Region, Malaysia*. CGPRT Centre

Thirumalai, K., P. N. DiNezio, Y. Okumura, and C. Deser (2017). Extreme Temperatures in Southeast Asia Caused by El Niño and Worsened by Global Warming. *Nature Communications*, **8**(1); 15531

WHO (2016). *World Health Organization*. World Health Organization

Xu, L., X. Xie, and S. Li (2013). Correlation Analysis of the Urban Heat Island Effect and the Spatial and Temporal Distribution of Atmospheric Particulates Using TM Images in Beijing. *Environmental Pollution*, **178**; 102–114

Yang, Q., X. Huang, and J. Li (2017). Assessing the Relationship Between Surface Urban Heat Islands and Landscape Patterns Across Climatic Zones in China. *Scientific Reports*, **7**(1); 1–11

Yang, S., Z. Li, J. Y. Yu, X. Hu, W. Dong, and S. He (2018). El Niño–Southern Oscillation and its Impact in the Changing Climate. *National Science Review*, **5**(6); 840–857

Yu, J.-Y., H. Paek, E. S. Saltzman, and T. Lee (2015). The Early 1990s Change in ENSO–PSA–SAM Relationships and its Impact on Southern Hemisphere Climate. *Journal of Climate*, **28**(23); 9393–9408

Zhang, Y., H. Balzter, B. Liu, and Y. Chen (2016). Analyzing the Impacts of Urbanization and Seasonal Variation on Land Surface Temperature Based on Subpixel Fractional Covers Using Landsat Images. *IEEE Journal of Selected Topics in Applied Earth Observations and Remote Sensing*, **10**(4); 1344–1356

Zhou, D., J. Xiao, S. Bonafoni, C. Berger, K. Deilami, Y. Zhou, S. Frolking, R. Yao, Z. Qiao, and J. A. Sobrino (2018). Satellite Remote Sensing of Surface Urban Heat Islands: Progress, Challenges, and Perspectives. *Remote Sensing*, **11**(1); 48

 